

ASSESSING THE SPATIOTEMPORAL URBAN GREEN COVER CHANGES AND THEIR IMPACT ON LAND SURFACE TEMPERATURE AND URBAN HEAT ISLAND IN LAHORE (PAKISTAN)

M. Jabbar*¹, M.M. Yusoff¹

¹University of Malaya, 50603 Kuala Lumpur, Malaysia

*Corresponding author: Jabbar.lhr@gmail.com

Received: January 12th, 2021 / Accepted: February 15th, 2022 / Published: March 31st, 2022

<https://DOI-10.24057/2071-9388-2021-005>

ABSTRACT. Urban vegetation has a decisive role in sustaining homogeneous Land Surface Temperature (LST) in a built-up environment. However, urban areas are facing rapid changes in land use/land cover (LULC) over the last few decades as green cover is being replaced by built-up structures. Consequently, LST is increasing and urban heat island (UHI) effects are expanding. In this context, this study was organized to assess urban green cover changes in Lahore and their impact on LST and UHI effects. For this, climate data was collected from the Pakistan Meteorological Department and Landsat images were acquired from Earth Explorer. LULC and LST maps were generated for 1990, 2000, 2010, and 2020 in ArcGIS 10.8. Also, Normalized Difference Vegetation Index (NDVI) and Normalized Difference Built-up Index (NDBI) were computed to analyze the effects of vegetation and built-up areas on LST and UHI. The study found that over the last three decades, built-up area increased 113.85% by removing 392.78 km² of green cover in the study area. Similarly, a rapid expansion of the high LST range and UHI effects was found towards the eastern and southern parts of the study area. Moreover, a negative correlation was found between LST and NDVI, whereas the correlation between LST and NDBI was found to be positive. Therefore, it was concluded that the continuation of green cover reduction is highly damaging because this might render the city more fragile ecologically. So, the study calls the attention of the responsible authorities for suitable measures against continuous green cover loss in the study area.

KEYWORDS: Land Surface Temperature; Land Use/Land Cover Changes; Urban Heat Island; Urban Green Cover; Normalized Difference Vegetation Index

CITATION: Jabbar M., Yusoff M. M. (2022). Assessing The Spatiotemporal Urban Green Cover Changes and Their Impact on Land Surface Temperature and Urban Heat Island in Lahore (Pakistan). Vol.15, Nº 1. Geography, Environment, Sustainability, p 122-140 <https://DOI-10.24057/2071-9388-2021-005>

ACKNOWLEDGEMENTS: *The author (Muhammad Jabbar) gratefully appreciates the support and supervision of the co-author (Dr. Mariney Mohd Yusoff) and the efforts of reviewers and editors in converting this piece of research into a successful scientific research paper.*

Conflict of interests: The authors reported no potential conflict of interest.

INTRODUCTION

Human life is strongly dependent on a suitable natural environment and cannot properly function without it. A balanced natural environment that exists on the earth makes it a suitable planet for living. However, human activities are continuously damaging the state of the natural environment. Urban green cover is significant for urban structure because it affects human life in many ways; for instance, urban green spaces stimulate better physical, psychological, and mental health and provide clean air for breathing. Besides the potential to reduce city temperature, the urban green cover offers healthy spaces for running, jogging, and walking. Urban green cover provides an appropriate environment for recreational and physical activities along with opportunities for social interaction (*WHO | Urban Green Spaces*, n.d.). Urban greenness is a well-recognized

element of socio-economic and environmental benefits. Physical, psychological, and emotional relaxation are all provided by urban green areas (Mensah et al. 2016).

Rapid urbanization and climate change created several challenges for urban residents. Rapid urbanization damages the urban environment, making it difficult to live in (Habitat, 2016). These rapid urban changes include the transformation of natural green places into impermeable surfaces, which increase Land Surface Temperature (land skin temperature that is derived from solar radiation) and Urban Heat Island (the region with a greater temperature than the surrounding environment) by shifting energy or radiation into the near-surface layer of the atmosphere (Aflaki et al. 2017; Forman, 2016; Oke, 1982). These Land Use / Land Cover (LULC) changes adversely affect the urban air quality and homogeneity of land surface temperature. The change of green cover into built-up spaces results in the emergence

and expansion of urban heat islands (Yu et al. 2018). Similarly, urban heat island negatively affects the urban environment as it aggravates air quality and increases energy and water consumption, which also has adverse effects on human and environmental health (Gunawardena et al. 2017; Varentsov et al. 2019; Wibowo et al. 2020; Zhang et al. 2017; Zhou et al. 2017). On the other side, urban vegetation reduces temperature, minimizes UHI effects, enhances air quality, conserves soil, reduces noise pollution, and cuts down wind speed (Lou et al. 2017). Urban green cover helps to mitigate climate change effects and provides a suitable environment for human and environmental well-being (Jabbar et al. 2021; Krellenberg et al. 2014).

All land cover types have distinct radiation and energy absorption capacities; therefore, it is crucial to consider them when modifying the physical properties of the earth's surface (Koko et al. 2021; Wang et al. 2017). Land cover modification disrupts the energy exchange pattern in the near-surface layer of the atmosphere. As a result, land use/land cover changes can significantly modify urban microclimate (Abuloye et al. 2015; Koko et al. 2021; Palafox-Juárez et al. 2021). Urban land cover modification particularly leads to high land surface temperature, which affects the thermal properties of the near-surface layer of the atmosphere. (Abuloye et al. 2015; Alavipanah et al. 2015; Jiang et al. 2015; Palafox-Juárez et al. 2021). Therefore, LST is recommended as an essential gauge for examining the earth heat balance or solar radiation budget. LST is a helpful indicator for identifying human-environment interaction because it regulates the bio-physical system of the earth (Kaplan et al. 2018; Palafox-Juárez et al. 2021).

Land use/land cover changes are a chief driver of environmental changes at the spatiotemporal scale (Mishra et al. 2014). LULC change detection is used to identify its temporal variation and helps to manage natural resources. Moreover, it provides valuable data on current land cover and a platform for future land use planning. Therefore, the assessment of LULC changes is a significant source of information for urban land use planning and sustainable development of the city (Naem et al. 2018; Yasin et al. 2019). In the recent decade, it has been observed that urban areas are expanding rapidly, especially in the developing world, and this trend is accompanied by significant changes in urban land cover settings, especially in the urban green cover (Fu & Weng 2016; Yasin et al. 2019). Therefore, it is important to assess urban green cover changes at a spatiotemporal scale and their effect on land surface temperature and urban heat island (Konstantinov et al. 2015).

Various studies have found that LULC changes are a major cause of the urban green cover reduction, and this reduction is

rapidly increasing in developing countries (El-Hattab et al. 2018; Koko et al. 2021; Palafox-Juárez et al. 2021; Ramaiah et al. 2020). Such a pattern of LULC change is highly significant because it affects land surface temperature. Because of this, it is crucial to examine the relationship between LULC changes and their effect on LST and UHI for urban planning and development. Furthermore, studies on the relationships between LULC changes and LST might be instrumental in an urban environment in the context of climate change (Mohamed, 2021). Deng et al. (2016), Jiang et al. (2015), Koko et al. (2021), and Palafox-Juárez et al. (2021) suggested that land surface temperature is a significant predictor of urban heat islands; therefore, an assessment of urban heat island can be made based on land surface temperature and NDVI data.

Lahore metropolitan is famed as a city of gardens. It is located in Pakistan, in a highly fertile area of the Upper Indus alluvial plain. Lahore is an economic hub of Pakistan and functions as a dry port for the whole country. This makes it an attractive place for living, which also leads to significant and rapid LULC changes (Shirazi & Kazmi 2016). The rapid development of built-up areas instead of green-covered land is damaging the ecosystem of the study area, converting it from a highly suitable place for living to an unsuitable one. The negligent behaviour of the management regarding the implementation of environmental guidelines in built-up areas and lack of accurate data are the main causes of environmental issues. Therefore, the assessment of urban green cover changes is necessary to identify the right pulse of land modification in the study area and overcome future environmental consequences. Under these considerations, this study was arranged to assess the urban green cover changes in Lahore and their effect on land surface temperature and urban heat island.

MATERIAL AND METHODS

The Study Area

Lahore is the second largest metropolitan area in Pakistan by population and the capital city of Punjab, which is the most populated province. It is located in the northeastern part of the province and extends from 31° 15' 0" N to 31° 45' 0" N and from 74° 01' 0" E to 74° 39' 0" E. According to the census report of 2017, the study area has 11,126,285 inhabitants. It covers an area of 1772 km² and has an average population density of 6278.94/km² (<https://pwd.punjab.gov.pk/>). Geographically, the study area is mostly located in the Upper Indus plain, particularly in the alluvial plain of the Ravi river, one of the Indus river tributaries.

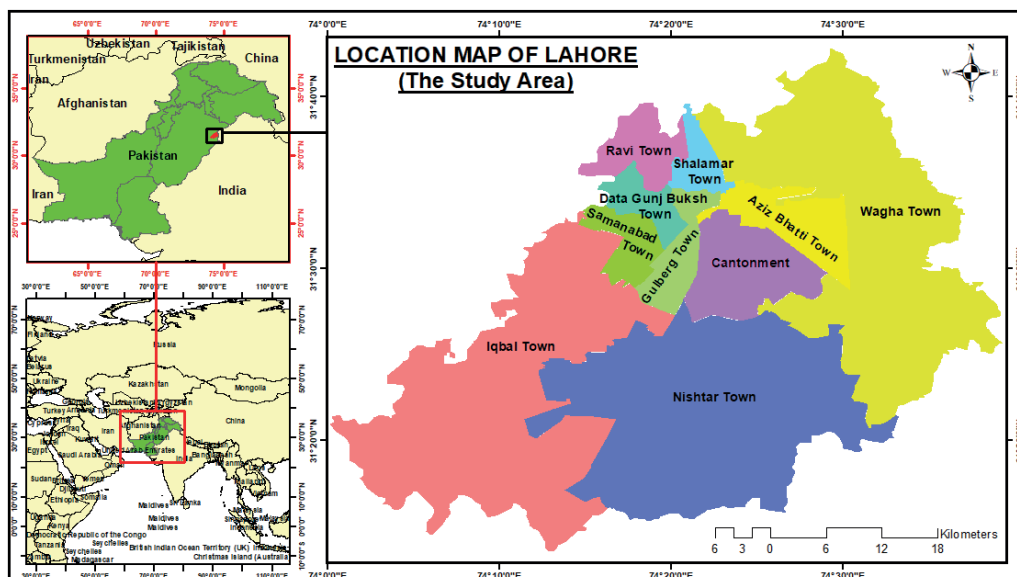


Fig. 1. Location of the Study Area

Climate of the Study Area

The study area is located in a semi-arid region characterized by five seasons: (i) Foggy Winter (from mid-November to mid-February with some western depression rainfall), (ii) Mild Spring (from mid-February to mid-May, (iii) Warm and Hot Summer (from mid-May to end-June with dust and rainy storms), (iv) Rainy Monsoon (from July to mid-September), and (v) Dry Autumn (from mid-September to mid-November). June is the hottest, July is the wettest, and January is the coldest month in the study area. The maximum recorded temperature is 48.3°C and

the minimum is -2.2°C (National Oceanic and Atmospheric Administration; Pakistan Meteorological Department).

The annual minimum temperature, which is presented in figure 3, varies from -2.2°C to 4°C. The temperature of -2.2°C was observed in the study area in 1996, 2006, and 2008, while 4°C was recorded in 2016. Regarding the change in the annual minimum temperature, the trendline shows a 0.4°C increase (0.5°C to 0.9°C) based on data for the last thirty years (1990 to 2019).

The annual maximum temperature in the study area, which is presented in figure 4, varies between 44°C and 48.8°C. The highest temperature (48.8°C) was observed in the study

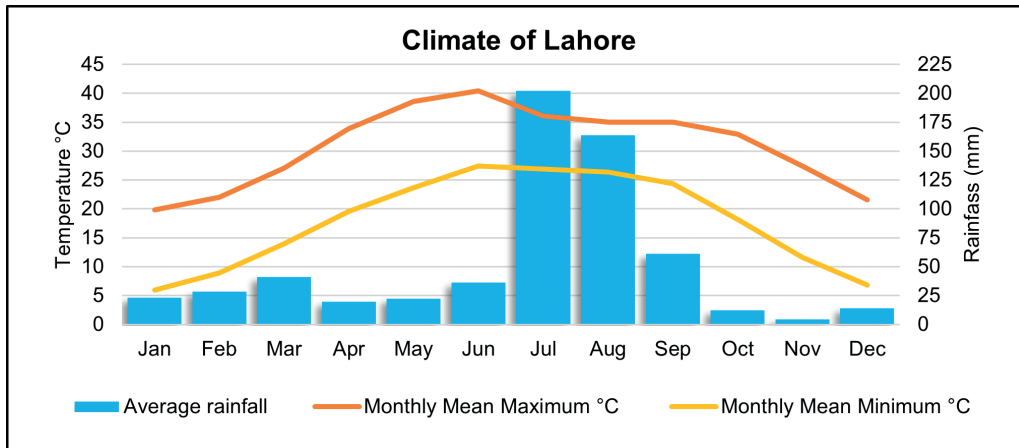


Fig. 2. Climate of the Study Area

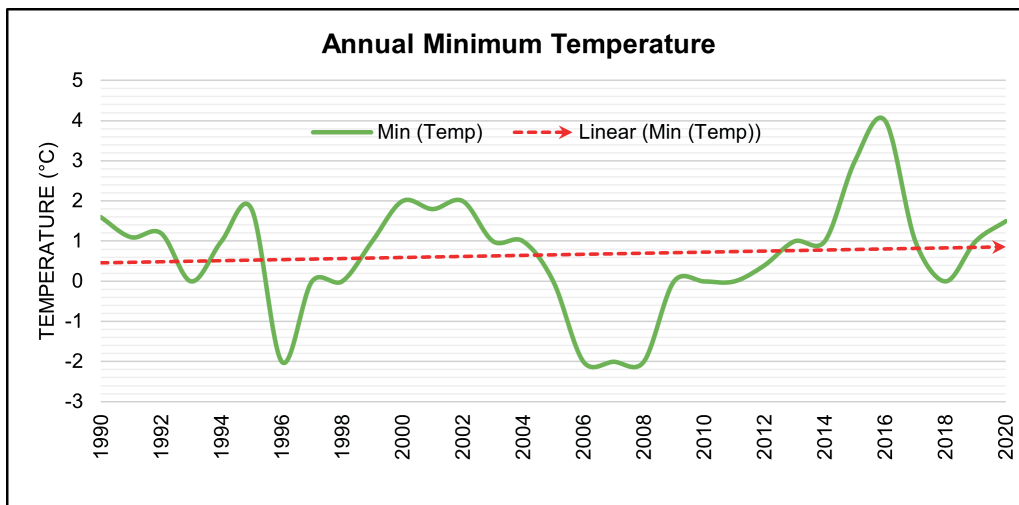


Fig. 3. Annual Minimum Temperature in the Study Area

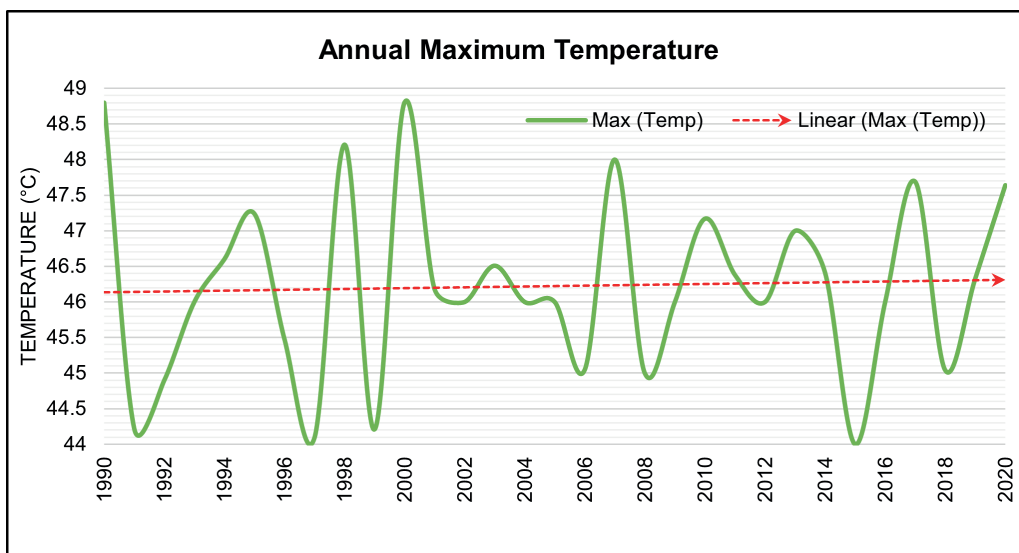


Fig. 4. Annual Maximum Temperature in the Study Area

area in 1990 and 2000. The trendline obtained from the analysis of changes in the annual maximum temperature shows an increase of 0.2°C. So, it was found that both annual minimum and maximum temperatures have increased in the study area.

Data Acquisition and Preparation

The study was based on Landsat images, which were acquired from Earth Explorer (<https://earthexplorer.usgs.gov/>) for the Path/Row 149/38. Spring was selected for the analysis as it is the most suitable season for LULC classification. The images were acquired for 16 March 1990, 19 March 2000, 7 March 2010, and 18 March 2020 according to the availability and clear weather conditions. All the acquired images had a resolution of 30 meters and are presented in table 1. During data preparation, the study area was extracted from the images by applying “extract by mask” tool in ArcGIS 10.8 after band composition.

LULC Classification

The study was based on Anderson’s Image Classification System (Level-I), which is used by the United States Geological Survey (USGS) in the LULC datasets. The study area was classified into five major land cover classes: (i) Forest Land, (ii) Agricultural Land, (iii) Barren Land, (iv) Built-up Area, and (v) Water Bodies. The Supervised Image Classification technique was applied for the classification. This Landsat image classification technique is characterized by the highest accuracy of the assessment (Barman et al. 2016; Iqbal & Iqbal 2018). After obtaining the classified images, the reclassification process was applied to clean misclassified cells using the cleanup tool. Then the classified image results were enhanced by removing the small isolated regions and smoothing class boundaries. After getting the final classified images, raster data was converted into polygons. Then the polygons were dissolved according to their class, and the area of each class was calculated by applying the geometry in the attribute

table. This procedure was repeated for the classification of all the images.

Accuracy Assessment

For the accuracy assessment, 450 random reference points were generated using Supervised Image Classifiers in ArcGIS. After that, the confusion (error) matrix and kappa statistics were calculated. Omission and Commission errors were also computed. Omission errors occur when a class pixel is included in other classes, while Commission error occurs when the system assigns pixels of a class that does not belong to this class. Moreover, the user’s and producer’s accuracy were calculated in the study.

The following equations were used during the accuracy assessment process:

$$\text{Producer’s Accuracy (\%)} = \left(\frac{X_{kk}}{X_{k+}} \right) X100 \tag{1}$$

$$\text{User’s Accuracy (\%)} = \left(\frac{X_{kk}}{X_{k+}} \right) X100\% \tag{2}$$

$$\text{Overall Accuracy (OA)} = \frac{1}{N} \sum_{k=1}^r n_i \tag{3}$$

$$\text{Kappa - coefficient (k)} = \frac{N \sum_{k=1}^r X_{kk} - \sum_{k=1}^r (X_{k+} \circ X_{+k})}{N^2 - \sum_{k=1}^r (X_{k+} \circ X_{+k})} \tag{4}$$

In these equations, *N* = Total No. of pixels, *r* = No. of classes, *X_{kk}* = Total pixels in a row, *X_{k+}* = Total samples in a row, and *X_{+k}* = Total samples in the column in the error matrix.

LULC Change Detection

A post-classification comparison technique was applied to detect the change between two classified images. All four self-classified images were used for the LULC change detection. The change (C) in land cover classes was calculated by applying equation 5.

Table 1. Detail of Landsat Images used in the study

Years	Satellite	Sensor	Path/Row	Resolution (m)	Acquisition Day
1990	Landsat-5	TM	149/38	30	16-03-1990
2000	Landsat-7	ETM	149/38	30	19-03-2000
2010	Landsat-7	ETM	149/38	30	07-03-2010
2020	Landsat-8	OLI	149/38	30	18-03-2020

Table 2. Accuracy of Classified Images

Class Name	1990		2000		2010		2020	
	U/A	P/A	U/A	P/A	U/A	P/A	U/A	P/A
Forest Land	84.48%	81.67%	89.66%	86.67%	89.47%	85.00%	91.38%	88.33%
Agricultural Land	90.65%	88.18%	92.73%	92.73%	92.04%	94.55%	93.75%	95.45%
Barren Land	89.83%	88.33%	90.00%	90.00%	86.89%	88.33%	93.10%	90.00%
Built-up Area	83.08%	90.00%	90.16%	91.67%	88.14%	86.67%	90.32%	93.33%
Water Bodies	90.91%	100%	100%	100%	100%	100%	100%	100%
	OA = 87.67%		OA = 91.00%		OA = 90.00%		OA = 92.67%	
	KC = 0.82		KC = 0.87		KC = 0.85		KC = 0.90	

Note: U/A = User’s Accuracy, P/A = Producer’s, O/A = Overall Accuracy, K/C = Kappa-coefficient

$$C_i = L_i - B_i \quad (5)$$

In the next step, the percentage of land cover changes (C %) was calculated using equation 6.

$$P_i = (L_i - B_i) / B_i \times 100 \quad (6)$$

Where i stands for No. of classes in the image, C_i represents the magnitude of changes in a class " i ", and P_i represents the percentage of change in classes.

Extraction of LST

Landsat 5 & 7

Land surface temperature was extracted using band 6 for Landsat 5 and 7, according to Chen et al. (2002). Firstly, digital numbers (DNs) of band 6 were converted into radiation luminance using equation 7. In this equation, QCALMIN is equal to 1, QCALMAX is equal to 255, QCAL stands for DN, whereas LMAX and LMIN are equal to 1 and 255, respectively.

$$\text{Radiance} = \frac{LMAX - LMIN}{QCALMAX - QCALMIN} (QCAL - QCALMIN) + LMIN \quad (7)$$

Secondly, LST in Kelvin was calculated using equation 8.

$$T = \frac{K2}{\ln(K1/L\gamma + 1)} \quad (8)$$

Lastly, temperature values in Kelvin (A) were converted into degrees Celsius (B) using equation 9.

$$B = A - 273.15 \quad (9)$$

Landsat 8

For the Landsat 8 image, land surface temperature was extracted using the following Metadata values: 0.10000 for Radiance add bands 10 & 11, 0.0003342 for Radiance Mult Band 10 & 11, 774.8853 for K1 constant band 10, 1321.0789 for K2, 480.8883 for K1 constant band 11, and 1201.1442 for K2.

By using the above values, LST was calculated from Landsat 8 in five stages:

(i) Thermal Infra-Red Digital Numbers were converted into TOA (Top of Atmosphere) spectral Radiance using equation 10.

$$L\lambda = ML \times QCAL + AL \quad (10)$$

(ii) Spectral radiance data were converted into TOA brightness temperature using equation 11.

$$BT = K2 / \ln(k1 / L\lambda + 1) - 272.15 \quad (11)$$

(iii) NDVI values were calculated using equation 12.

$$NDVI = (NIR - RED) / (NIR + RED) \quad (12)$$

(iv) Average Land Surface Emissivity (LSE) was determined using equations 13 and 14, in which PV is the proportion of vegetation, and E is Land Surface Emissivity.

$$PV = (NDVImax - NDVImin) / (NDVImax + NDVImin) \wedge 2 \quad (13)$$

$$E = 0.004 * PV + 0.986 \quad (14)$$

(v) LST was calculated using equation 15.

$$LST = (BT / 1) + W * (BT / 14380) * \ln(E) \quad (15)$$

After generating the LST maps, the areas of each LST range were calculated in QGIS 3.14.

Quantification of NDVI, NDBI, and UHI

NDVI was quantified using equation 12, whereas for NDBI equation 16 was applied.

$$NDBI = (SWIR - NIR) / (SWIR + NIR) \quad (16)$$

After that, the relationships of LST with NDVI and NDBI were analyzed using Fishnet Polygons, and then the data from LST, NDVI, and NDBI maps were extracted.

UHI was quantified in ArcGIS 10.8 using equation 17 based on LST maps of 1990 and 2020.

$$UHI = (Ts - Tm) / SD \quad (17)$$

Two UHI profiles were calculated: (i) North to South and (ii) West to East, creating the polylines in both directions using Stack Profiles.

RESULTS

Land Use/Land Covers Changes

Land use/land cover changes in the study area were detected using Landsat images of 1990, 2000, 2010, and 2020, as shown in figure 5. The figure shows that the study area has faced rapid LULC changes in the last three decades. In 1990, the study area had 23.41% of Forest Land, 48.03% of Agricultural Land, 11.18% of Barren Land, 16.17% of Built-up Area, and 1.21% Water Bodies. However, after ten years, in 2000, the distribution in the study area changed to 17.30% of Forest Land, 46.09% of Agricultural land, 14.38% of Barren Land, 21.38% of Built-up Area, and 0.83% of Water Bodies. Consequently, the share of Forest Land in the study area decreased over this decade (1990 to 2000) by 6.11%, Agricultural Land decreased by 1.94%, while Barren Land and Built-up Area increased by 3.20% and 5.21%, respectively, the share of Water Bodies also decreased by 0.38%.

After assessing the LULC changes from 1990 to 2000, LULC for 2010 was analyzed. It was found that in this year, the study area had 14.79% of Forest Land, 42.18% of Agricultural Land, 16.59% of Barren Land, 25.73% of Built-up Area, and 0.69% of Water Bodies. As a result, in the decade from 2000 to 2010, the share of Forest Land and Agricultural Land in the study area further decreased by 2.51% and 3.91%, respectively, while Barren Land increased by 2.21%, Built-up Area increased by 4.35%, and Water Bodies decreased by 0.14%.

In order to analyze LULC changes over three decades (1990 to 2020), LULC was also detected for 2020. It was found that in the final year, the study area had 11.97% of Forest Land, 37.31% of Agricultural Land, 15.29% of Barren Land, 34.58% of Built-up Area, and 0.85% of Water Bodies. As a result, in the third decade (2010 to 2020) the share of Forest Land, Agricultural Land and Barren Land decreased by 2.82%, 4.87% and 1.30%, respectively, while Built-up Area increased by 8.85%, and Water Bodies increased by 0.16% in.

As expected, it was found that in the last three decades (1990 to 2020), the share of Forest Land decreased by 11.44% (from 23.41% to 11.97%), Agricultural Land decreased by 10.72% (from 48.03% to 37.31%), and Water Bodies decreased by 0.36% (from 1.21% to 0.85%). On the other side, the area of Barren Land and Built-up Area increased during the last three decades by 4.11% (from 11.18% to 15.29%), and 18.41% (from 16.17% to 34.58%), respectively. Finally, it was confirmed that a rapid increase in Built-up Area occurred along with a swift decrease in Forest Land, which is the main concern of the study as it directly affects LST and UHI. All the details of land use/land cover changes are given in figure 5.

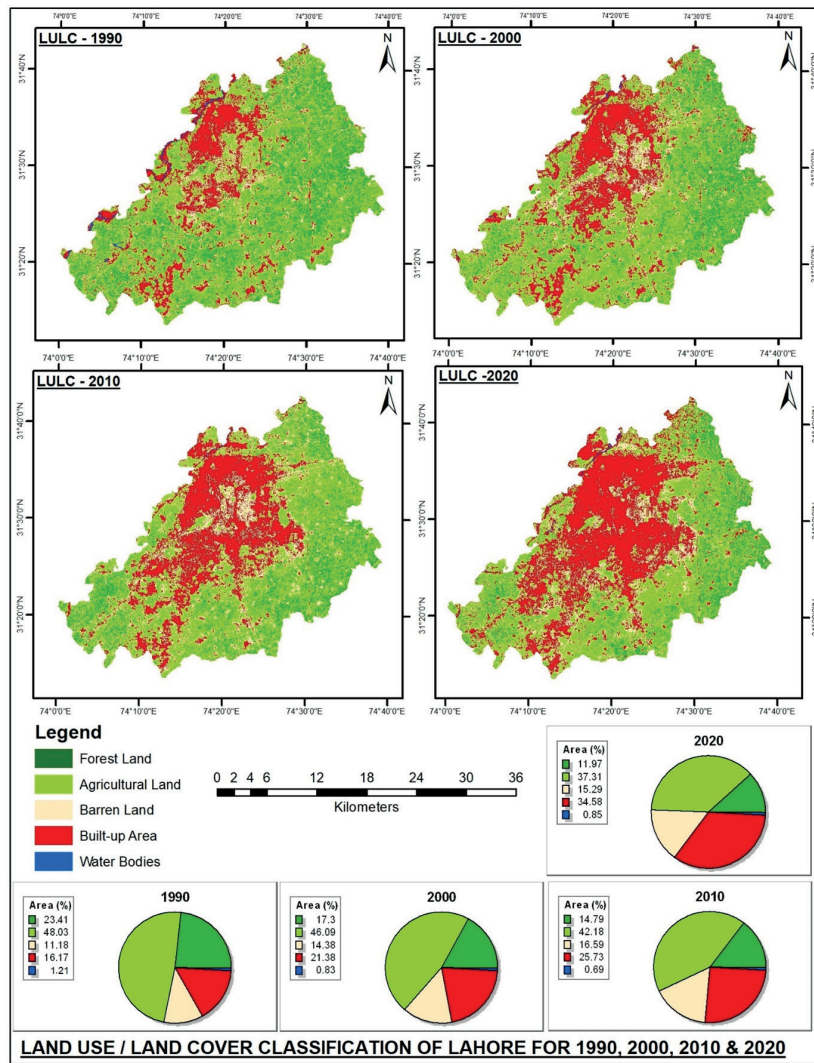


Fig. 5. Land Use/Land Cover Classification of the Study Area

Changes in Land Cover Area

After assessing the LULC changes over three decades (1990 to 2020), it was found that the decrease in area corresponded only to green and blue land cover types whereas the area of built-up and barren land increased. Figure 6 shows the overall increase and decrease in area of different land cover types. It can be seen that the area of Forest Land, Agricultural Land, and Water Bodies lost 202.72 km² (11.44%),

189.96 km² (10.72%), and 6.38 km² (0.36%), whereas Barren Land and Built-up Area gained 72.83 km² (4.11%) and 326.23 km² (18.41%) respectively.

Changes in Land Surface Temperature

The change of green cover into built-up environment was found to be a significant cause of LST increase and UHI development in various studies (Amani-Beni et al. 2019;

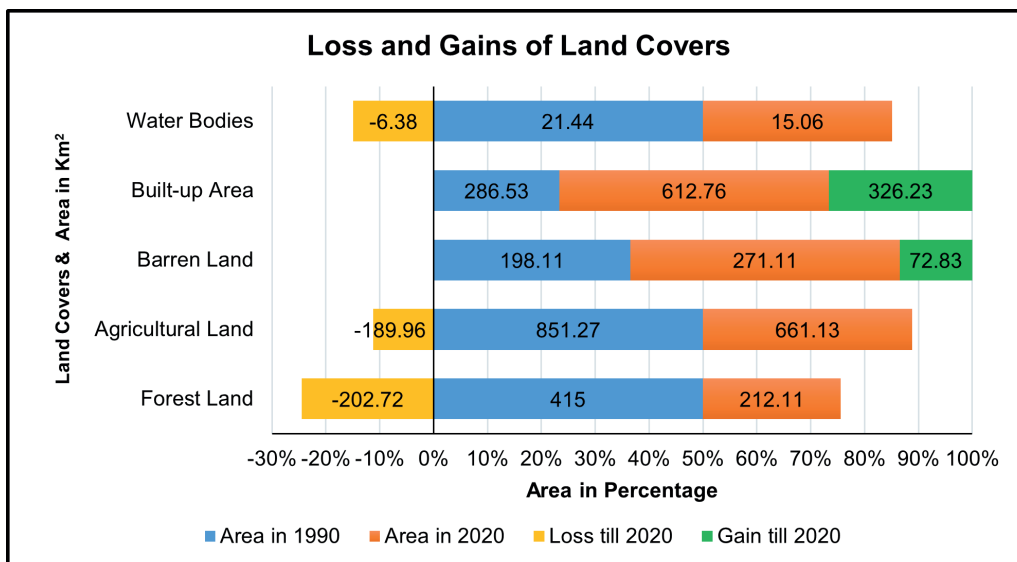


Fig. 6. Loss and Gains of Land Covers from 1990 to 2020

Wan Mohd Jaafar et al. 2020; Yu et al. 2018). Therefore, LST was also computed for the study area. It is shown in figure 07, which presents seven land surface temperature ranges; (i) 14°C - 21°C, (ii) 21°C - 22°C, (iii) 22°C - 23°C, (iv) 23°C - 24°C, (v) 24°C - 25°C, (vi) 25°C - 26°C, and (vii) 26°C - 32°C for 1990, 2000, 2010, and 2020.

The comparison of these LST ranges showed that the area under the first LST range (14°C - 21°C) amounted to 0.20% of the total area in 1990, 8.31% in 2000, 2.29% in 2010 and 6.68% in 2020, so a slight overall area expansion was found for this range. Similarly, an increase was found in the area under the second LST range (21°C - 22°C) as it stood at 11.60% in 1990, 26.56% in 2000, 37.39% in 2010, and 20.44% in 2020. The area under the third LST range (22°C - 23°C) reduced as it amounted to 29.12% in 1990, 20.20% in 2000, 20.66% in 2010, and 19.27% in 2020. For the fourth LST range (23°C - 24°C), a significant expansion was found with the area changing from 36.73% in 1990, to 13.54% in 2000, 16.48% in 2010, and 8.74% in 2020. Similarly, a slight expansion was found for the fifth LST range (24°C - 25°C) as its area accounted for 17.94% of the total area in 1990, 19.90% in 2000, 8.25% in 2010, and 20.38% in 2020. A considerable expansion was found for the sixth LST range (25°C - 26°C). Its area changed from 3.23% in 1990, to 8.84% in 2000, 10.42% in 2010, and 14.12% in 2020. Almost similar results were found for the seventh and last LST range (26°C - 32°C). The area under this range amounted to 0.55% in 1990, 2.02% in 2000, 1.87% in 2010 and 9.73% in 2020. The results of the LST comparison show that the ranges with

the highest land surface temperature (sixth and seventh) expanded sharply and constantly, which represents a considerable change in the land surface temperature of the study area.

Correlation of LST with NDVI and NDBI

The correlation of LST with NDVI and NDBI is shown in figure 8. A negative relationship was found between LST and NDVI, whereas between LST and NDBI it was positive. According to these relationships, higher NDVI leads to lower LST, and lower NDVI leads to higher LST. A 5°C decrease in LST corresponds to the increase of NDVI by 0.5. On the other hand, a positive relationship between LST and NDBI means that LST increases with NDBI increase and decreases with the decreasing NDBI. The trendline shows that more than 5°C increase in LST corresponds to an increase of NDBI from -0.35 to 0.1. From these results, it is clear that LST decreases with increasing NDVI and decreasing NDBI. Similarly, LST increases with decreasing NDVI and increasing NDBI. This correlation proves that urban green cover may contribute to a 5°C LST decrease and can help to maintain thermal homogeneity in cities.

Urban Heat Island

Urban Heat Island effects are commonly found in urban areas, especially in developing countries like Pakistan. These effects become broader and more severe with the

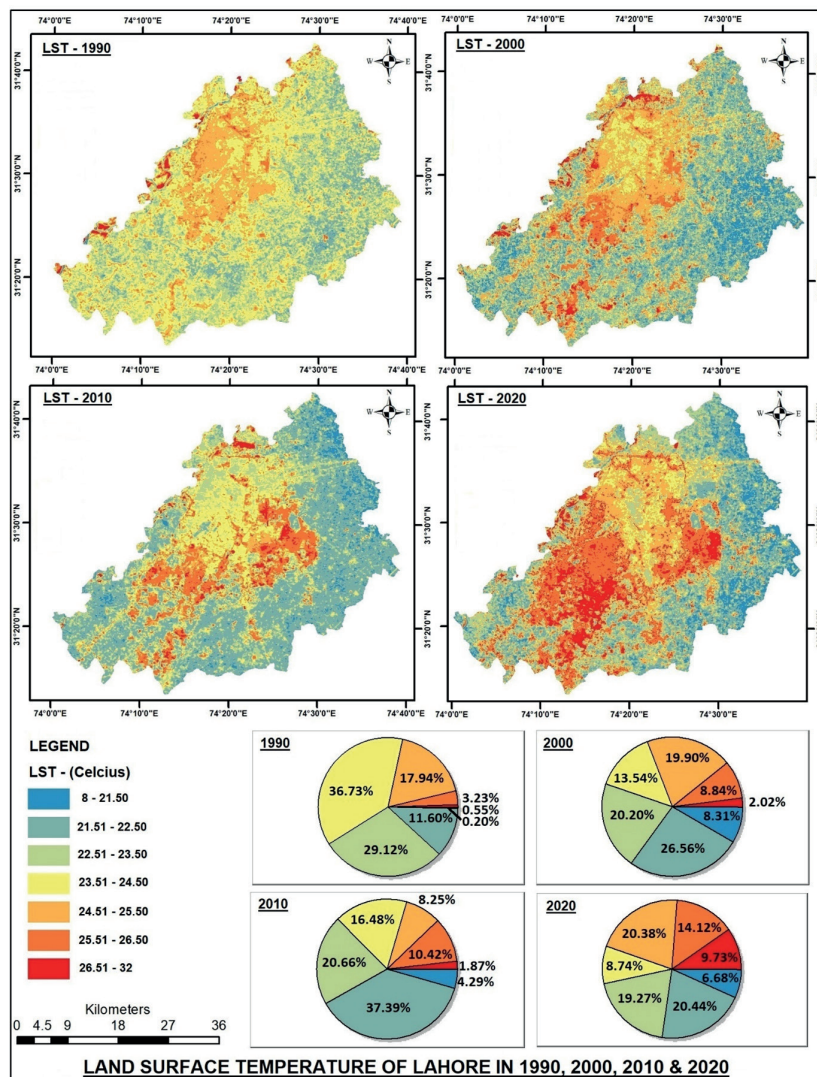


Fig. 7. Changes in Land Surface Temperature in the Study Area

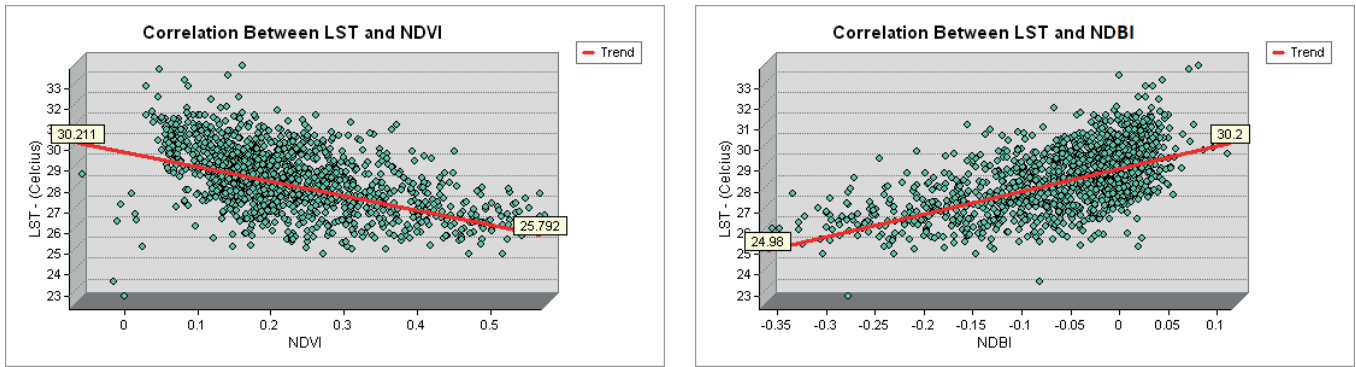


Fig. 8. Correlation of LST with NDVI and NDBI

expansion of urban built-up areas. In this context, the UHI of Lahore was analyzed for the years 1990 and 2020. Figure 9 shows the UHI profiles of the study area in which 1990-(A) and 2020-(A) display North to South profiles, whereas 1990-(B) and 2020-(B) show West to East profiles. The comparison of these UHI profiles is presented below.

UHI-1990-(A) shows LST fluctuations from 19°C to 27°C. A decreasing trend can be found between 20,000 and 32,500 meters as LST drops from 23°C to 19°C. After that, LST increases again reaching 23°C. The low LST area consists of green cover, which confirms the negative relation between green cover and LST. This profile is compared to UHI-2020-(A), which presents LST along the same axis. The UHI-2020-(A) shows high LST from 5,000 to 8,000 meters and from 19,000 meters to the end of the study area. Between 8,000 and 19,000 meters, LST is more or less constant, which is similar to UHI-1990-(A). This UHI comparison shows an LST increase in UHI-2020-(A) where green cover was replaced with built-up area (19,000 to 38,000 meters). This demonstrates an evident expansion of UHI due to the removal of green cover.

UHI-1990-(B) and UHI-2020-(B) represent West to East UHI profiles of the study area. UHI-1990-(B) shows LST around 21 to 22°C from 1,000 to 5,000 meters, but after that, it fluctuates around 23°C from 5,000 to 22,000 meters. Next, a decreasing trend was found from 22,000 to 26,000 meters as LST drops from 23°C to 20°C. After that, LST is almost constant between 26,000 and 41,000 meters. For UHI-2020-(B) an increasing trend was found between 5,000 and 20,000 meters where LST changes from 27 to 29°C, while in UHI-1990-(B) it was 23°C. Similarly, higher LST was found from 25,000 to 40,000 meters. Overall, the high LST area in 2020 was found from 5,000 to 40,000 meters, while

in 1990 it spanned from 5,000 to 21,000 meters, which suggests that UHI has expanded by almost 19,000 meters in the last thirty years. So, after comparing UHI profiles from north to south and from west to east for the years 1990 and 2020, there is an evident indication of UHI expansion with the built-up area increase.

DISCUSSION

The effect of Land Use/Land Cover changes is not limited to Land Surface Temperature as they also affect air temperature. In this study, it was found that LST and UHI effects increased with the replacement of green cover by built-up area. Also, an increasing trend was found for the annual maximum and minimum (air) temperature in the study area. Similar results were found in various other studies. Yang et al. (2013) conducted a study in Anhui Province of China and found that annual mean maximum and minimum temperature increased by 0.407, 0.383, and 0.432°C per decade from 1970 to 2008 due to LULC changes (Yang et al. 2013). So, the results of this study support the assertion that the study area has become warmer due to the loss of urban green cover and rapid growth of built-up area. The impact of LULC changes on air temperature was also analyzed in other studies. A regional study on East Asia projected an 0.14°C air temperature increase between 2030 to 2060 due to LULC changes (Niu et al. 2019). It was shown that air temperature also increases along with LST due to the urban expansion and removal of urban green cover. LULC changes led to the increase in air temperature in Beijing–Tianjin–Hebei. The conversion of cropland into built-up area was found to be the most significant factor, causing an 0.36°C/decade increase in air temperature,

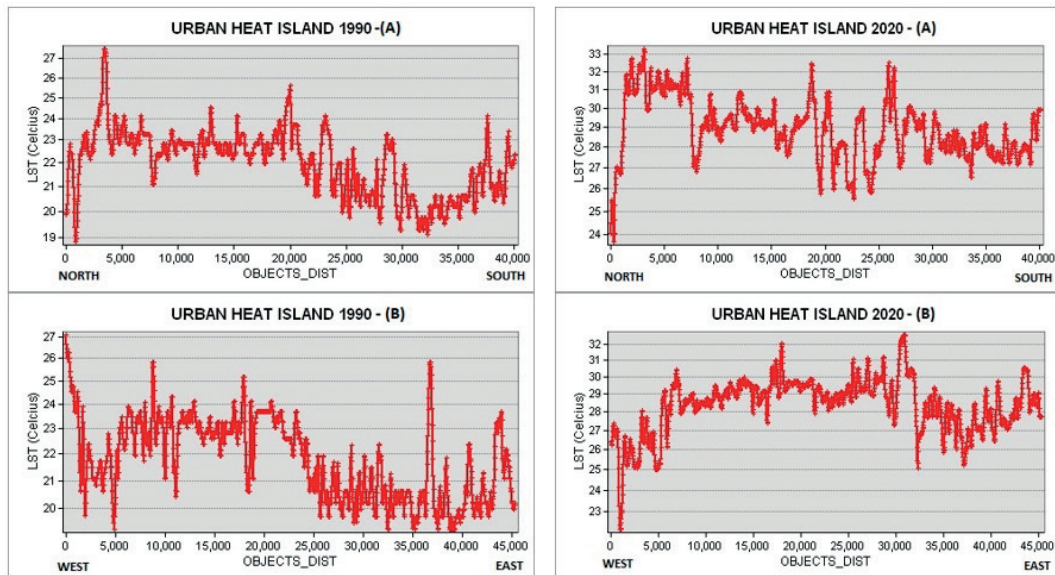


Fig. 9. Comparison of the Urban Heat Island in 1990 and 2020

while the changes from grassland to built-up area led to an $0.306^{\circ}\text{C}/\text{decade}$ increase (Li et al. 2018, p.). Similarly, built-up land in the study area is expanding due to the removal of Forest and Agricultural Land, which leads to increasing air and land surface temperature trend. So, the results of this study support the statement that urban green cover works as a ventilator that maintains urban temperature and reduces UHI effects.

From the comparison of LST profiles (i) UHI-1990-A and UHI-2020-A and (ii) UHI-1990-B and UHI-2020-B, it was found that UHI effects expanded in the study area towards its southern and eastern parts. The area of moderate LST range has also shifted towards high LST, for example, 26°C - 32°C (the highest) LST range covered only 0.20% of the total area in 1990, while in 2020 it amounted to 9.73%. It means that the area of the maximum temperature zone has significantly increased and the UHI effect expanded with the decrease in green cover and increase in built-up area. Similar findings were given by Forman (2016), stating that rapid modification of green spaces into impermeable surfaces increases the reflection of solar radiation energy into the near-surface layer of the atmosphere. Also, Yu et al. (2017) concluded that built-up area expansion is a significant cause of the UHI development (Yu et al. 2018). UHI has several adverse effects on the urban environment, including the increase in energy consumption and water usage (Gunawardena et al. 2017; Zhang et al. 2017; Zhou et al. 2017). The expansion of UHI in the study area will also result in higher energy and water usage, which will ultimately lead to higher LST and air temperature. Therefore, the study highlights that the loss of green cover enhances extreme environmental issues like harsh UHI effects and high LST, especially during summer.

The study area is located in a semi-arid region, which means that the amount of natural vegetation is already lower than required. Under these circumstances, green cover in the study area becomes even more valuable. In contrast, the results show a significant decrease in the urban green cover area (Forest Land and Agricultural Land). The green cover in the study area is shrinking, whereas built-up area is expanding rapidly. In the last three decades, the study area lost 1/3 of its green area, which was replaced by impermeable surfaces as built-up area increased more than 100%. These changes are severe because the decrease of green cover still continues without any restriction.

The study also analyzed relationships of LST with NDVI and NDBI to recognize the actual effects of vegetation and built-up area on LST and UHI. The results (figure 08) show that LST is negatively correlated with NDVI. High NDVI leads to lower LST and reduces the UHI effects, whereas low NDVI causes LST increase and enhances the UHI effects. On the other side, the relationship between LST and NDBI was found to be positive, indicating that expansion of built-up area leads to the expansion of UHI and higher LST. In all study areas, the decrease in NDVI comes with a decrease in plant cover and an increase in the natural environment changes. According to the findings, vegetation regions

and areas outside built-up sites have greater NDVI and lower LST. Low LST was found in regions with dense natural plant cover and gardens as well as in fields of dense agricultural vegetation with high NDVI values. Vegetation helps to reduce LST through evapotranspiration (Grover & Singh, 2015; Palafox-Juárez et al. 2021). These findings also correspond with similar studies based on Landsat data analysis (Guo et al. 2019; Kaplan et al. 2018; Tran et al. 2017). The matter is more threatening because the built-up land cover is still expanding towards the remaining green area, increasing the area of dark surfaces in the city, which causes an increase in air and land surface temperature. With increasing land surface and air temperature, the UHI effects will be more severe in the future. The study area is also located in a semi-arid region and faces extreme temperatures up to 48°C in the summer season, as well as more than 50°C feels like temperature in wet summer. In these circumstances, the availability of green spaces in highly built-up areas is needed because they work like a ventilator and decrease the temperature by almost 5°C .

CONCLUSION AND SUGGESTIONS

The study analyzed urban green cover reduction in Lahore due to LULC changes and found its significant effects on LST and UHI expansion. It was found that the study area is continuously losing its green cover due to rapid urban expansion. LULC changes have demolished a significant part of urban green cover, whereas built-up areas and barren land have spread over 50% of the total area without any planning and violating environmental guidelines. Rapid urban expansion has led to a large-scale increase in the area of dark surfaces in the city, which is accelerating land surface temperature increase and enhancing the UHI effects. The trends of increasing air temperature and LST are attracting extreme climatic events towards the study area. The expansion of built-up area in place of agricultural and forest land has led to the green cover removal, which expanded high LST and UHI effects towards the eastern and southern parts of the study area.

The continuation of the found LULC change trend is extremely sensitive for the ecosystem and ecological structure of the study area. These changes might render the city more ecologically fragile, particularly the areas that could be transformed into built-up regions in the future. So, more studies are needed to evaluate vegetation cover required for a sustainable environment of the city and mitigation of global climate change effects at the micro-level. Moreover, studies are required to convert the high heated built-up land into sustainable and thermally homogeneous areas by using modern technologies like green walls, green roofs, and vertical gardens. Finally, the study calls the attention of the management to mitigate or minimize the adverse effects of LULC changes by limiting the loss of green cover and increasing the number of green spaces in densely populated urban areas, which would help to reduce LST and UHI effects in the city. ■

REFERENCES

- Abuloye, A., Popoola, K., Adewale, A., Vera, O., & Nicholas, E. (2015). Assessment of Daytime Surface Urban Heat Island in Onitsha, Nigeria, DOI: 10.13140/RG.2.1.5117.5765.
- Aflaki A., Mirnezhad M., Ghaffarianhoseini A., Ghaffarianhoseini A., Omrany H., Wang Z.-H., & Akbari H. (2017). Urban heat island mitigation strategies: A state-of-the-art review on Kuala Lumpur, Singapore and Hong Kong. *Cities*, 62, 131–145.
- Alavipanah S., Wegmann M., Qureshi S., Weng Q., & Koellner T. (2015). The Role of Vegetation in Mitigating Urban Land Surface Temperatures: A Case Study of Munich, Germany during the Warm Season. *Sustainability*, 7(4), 4689–4706. <https://doi.org/10.3390/su7044689>
- Amani-Beni M., Zhang B., Xie G.-D., & Shi Y. (2019). Impacts of urban green landscape patterns on land surface temperature: Evidence from the adjacent area of Olympic Forest Park of Beijing, China. *Sustainability*, 11(2), 513.

- Barman T., Ghongade R., & Ratnaparkhi A. (2016). Rough set based segmentation and classification model for ECG. 2016 Conference on Advances in Signal Processing (CASP), 18–23.
- Deng X., Li, Z., & Gibson J. (2016). A review on trade-off analysis of ecosystem services for sustainable land-use management. *Journal of Geographical Sciences*, 26(7), 953–968.
- El-Hattab M., S.m. A., & G.e. L. (2018). Monitoring and assessment of urban heat islands over the Southern region of Cairo Governorate, Egypt. *The Egyptian Journal of Remote Sensing and Space Science*, 21(3), 311–323, DOI: /10.1016/j.ejrs.2017.08.008.
- Forman R. T. (2016). Urban ecology principles: Are urban ecology and natural area ecology really different? *Landscape Ecology*, 31(8), 1653–1662.
- Fu P., & Weng Q. (2016). A time series analysis of urbanization induced land use and land cover change and its impact on land surface temperature with Landsat imagery. *Remote Sensing of Environment*, 175, 205–214.
- Grover A., & Singh R. B. (2015). Analysis of Urban Heat Island (UHI) in Relation to Normalized Difference Vegetation Index (NDVI): A Comparative Study of Delhi and Mumbai. *Environments*, 2(2), 125–138, DOI:10.3390/environments2020125.
- Gunawardena K. R., Wells M. J., & Kershaw T. (2017). Utilising green and bluespace to mitigate urban heat island intensity. *Science of the Total Environment*, 584, 1040–1055.
- Guo G., Wu Z., & Chen Y. (2019). Complex mechanisms linking land surface temperature to greenspace spatial patterns: Evidence from four southeastern Chinese cities. *Science of The Total Environment*, 674, 77–87.
- Iqbal M. Z., & Iqbal M. J. (2018). Land use detection using remote sensing and gis (A case study of Rawalpindi Division). *American Journal of Remote Sensing*, 6(1), 39–51.
- Jabbar M., Yusoff M. M., & Shafie A. (2021). Assessing the role of urban green spaces for human well-being: A systematic review. *GeoJournal*, DOI:10.1007/s10708-021-10474-7.
- Jiang Y., Fu, P., & Weng Q. (2015). Assessing the Impacts of Urbanization-Associated Land Use/Cover Change on Land Surface Temperature and Surface Moisture: A Case Study in the Midwestern United States. *Remote Sensing*, 7(4), 4880–4898. <https://doi.org/10.3390/rs70404880>
- Kaplan G., Avdan U., & Avdan Z. Y. (2018). Urban Heat Island Analysis Using the Landsat 8 Satellite Data: A Case Study in Skopje, Macedonia. *Proceedings*, 2(7), 358, DOI:10.3390/ecrs-2-05171.
- Koko A. F., Yue W., Abubakar G. A., Alabsi A. A. N., & Hamed R. (2021). Spatiotemporal Influence of Land Use/Land Cover Change Dynamics on Surface Urban Heat Island: A Case Study of Abuja Metropolis, Nigeria. *ISPRS International Journal of Geo-Information*, 10(5), 272, DOI: 10.3390/ijgi10050272.
- Konstantinov P. I., Grishchenko M. Y., & Varentsov M. I. (2015). Mapping urban heat islands of arctic cities using combined data on field measurements and satellite images based on the example of the city of Apatity (Murmansk Oblast). *Izvestiya, Atmospheric and Oceanic Physics*, 51(9), 992–998, DOI: 10.1134/S000143381509011X.
- Krellenberg K., Welz J., & Reyes-Päcke S. (2014). Urban green areas and their potential for social interaction—A case study of a socio-economically mixed neighbourhood in Santiago de Chile. *Habitat International*, 44, 11–21, DOI: 10.1016/j.habitatint.2014.04.004.
- Li J., Zheng X., Zhang C., & Chen Y. (2018). Impact of land-use and land-cover change on meteorology in the Beijing–Tianjin–Hebei Region from 1990 to 2010. *Sustainability*, 10(1), 176.
- Lou H., Yang S., Zhao C., Wang Z., Liu X., Shi L., Wu L., Hao F., & Cai M. (2017). Combining multi-source data to explore a mechanism for the effects of micrometeorological elements on nutrient variations in paddy land water. *Paddy and Water Environment*, 15(3), 513–524, DOI: 10.1007/s10333-016-0568-5.
- MAHMOUDZADEH H. (2007). Digital change detection using remotely sensed data for monitoring green space destruction in Tabriz.
- Mensah C. A., Andres L., Perera U., & Roji A. (2016). Enhancing quality of life through the lens of green spaces: A systematic review approach. *International Journal of Wellbeing*, 6(1), 142–163, DOI: 10.5502/ijw.v6i1.445.
- Mishra V. N., Rai P. K., & Mohan K. (2014). Prediction of land use changes based on land change modeler (LCM) using remote sensing: A case study of Muzaffarpur (Bihar), India. *Journal of the Geographical Institute» Jovan Cvijic», SASA*, 64(1), 111–127.
- Mohamed M. A. (2021). Spatiotemporal Impacts of Urban Land Use/Land Cover Changes on Land Surface Temperature: A Comparative Study of Damascus and Aleppo (Syria). *Atmosphere*, 12(8), 1037, DOI: 10.3390/atmos12081037.
- Naeem M. A., Armutlulu A., Imtiaz Q., Donat F., Schäublin R., Kierzkowska A., & Müller C. R. (2018). Optimization of the structural characteristics of CaO and its effective stabilization yield high-capacity CO₂ sorbents. *Nature Communications*, 9(1), 1–11.
- National Oceanic and Atmospheric Administration. (n.d.). Retrieved 5 October 2020, from <https://www.noaa.gov/>
- Niu X., Tang J., Wang S., & Fu C. (2019). Impact of future land use and land cover change on temperature projections over East Asia. *Climate Dynamics*, 52(11), 6475–6490, DOI: 10.1007/s00382-018-4525-4.
- Oke T. R. (1982). The energetic basis of the urban heat island. *Quarterly Journal of the Royal Meteorological Society*, 108(455), 1–24.
- Pakistan Meteorological Department PMD. (n.d.). Retrieved 5 October 2020, from <http://www.pmd.gov.pk/index-old.html>
- Palafox-Juárez E. B., López-Martínez J. O., Hernández-Stefanoni J. L., & Hernández-Nuñez H. (2021). Impact of Urban Land-Cover Changes on the Spatial-Temporal Land Surface Temperature in a Tropical City of Mexico. *ISPRS International Journal of Geo-Information*, 10(2), 76, DOI: 10.3390/ijgi10020076.
- Ramaiah M., Avtar R., & Rahman M. M. (2020). Land Cover Influences on LST in Two Proposed Smart Cities of India: Comparative Analysis Using Spectral Indices. *Land*, 9(9), 292, DOI: 10.3390/land9090292.
- Shirazi S. A. (n.d.). Temporal Analysis of Land Use and Land Cover Changes in Lahore-Pakistan. 13(1), 20.
- Shirazi S. A., & Kazmi J. H. (2016). Analysis of socio-environmental impacts of the loss of urban trees and vegetation in Lahore, Pakistan: A review of public perception. *Ecological Processes*, 5(1), 1–12.
- Tran D. X., Pla F., Latorre-Carmona P., Myint S. W., Caetano M., & Kieu H. V. (2017). Characterizing the relationship between land use land cover change and land surface temperature. *ISPRS Journal of Photogrammetry and Remote Sensing*, 124, 119–132, DOI: 10.1016/j.isprsjprs.2017.01.001.
- Varentsov M. I., Grishchenko M. Y., & Wouters H. (2019). Simultaneous assessment of the summer urban heat island in Moscow megacity based on in situ observations, thermal satellite images and mesoscale modeling. *GEOGRAPHY, ENVIRONMENT, SUSTAINABILITY*, 12(4), 74–95, DOI: 10.24057/2071-9388-2019-10.
- Wan Mohd Jaafar W. S., Abdul Maulud K. N., Muhmad Kamarulzaman A. M., Raihan A., Md Sah S., Ahmad A., Saad S. N. M., Mohd Azmi A. T., Jusoh Syukri N. K. A., & Razaq Khan W. (2020). The influence of deforestation on land surface temperature—A case study of Perak and Kedah, Malaysia. *Forests*, 11(6), 670.
- Wang H., Zhang Y., Tsou J. Y., & Li Y. (2017). Surface Urban Heat Island Analysis of Shanghai (China) Based on the Change of Land Use and Land Cover. *Sustainability*, 9(9), 1538, DOI: 10.3390/su9091538.

WHO | Urban green spaces. (n.d.). WHO; World Health Organization. Retrieved 27 April 2020, from <http://www.who.int/sustainable-development/cities/health-risks/urban-green-space/en/>

Wibowo A., Yusoff M. M., Adura T. A., & Zaini L. H. (2020). Spatial model of air surface temperature using Landsat 8 TIRS. *IOP Conference Series: Earth and Environmental Science*, 500(1), 012009.

Yang Y.-J., Wu B.-W., Shi C., Zhang J.-H., Li Y.-B., Tang W.-A., Wen H.-Y., Zhang H.-Q., & Shi T. (2013). Impacts of Urbanization and Station-relocation on Surface Air Temperature Series in Anhui Province, China. *Pure and Applied Geophysics*, 170(11), 1969–1983, DOI: 10.1007/s00024-012-0619-9.

Yasin M. Y., Yusof M., & Nisfariza M. N. (2019). Urban sprawl assessment using time-series lulc and NDVI variation: A case study of Sepang, Malaysia. *Applied Ecology and Environmental Research*, 17(3), 5583–5602.

Yu Z., Guo X., Zeng Y., Koga M., & Vejre, H. (2018). Variations in land surface temperature and cooling efficiency of green space in rapid urbanization: The case of Fuzhou city, China. *Urban Forestry & Urban Greening*, 29, 113–121.

Zhang L., Tan P. Y., & Diehl J. A. (2017). A conceptual framework for studying urban green spaces effects on health. *Journal of Urban Ecology*, 3(1), DOI: 10.1093/jue/jux015.

Zhou W., Wang J., & Cadenasso M. L. (2017). Effects of the spatial configuration of trees on urban heat mitigation: A comparative study. *Remote Sensing of Environment*, 195, 1–12.